Regular Article

Electrodeposition of Ginseng/Polyaniline Encapsulated Poly(lactic-*co*-glycolic Acid) Microcapsule Coating on Stainless Steel 316L at Different Deposition Parameters

Siti Khadijah Lukman,[a] Rania Hussein Al-Ashwal,[a] Naznin Sultana,[a] and Syafiqah Saidin*[,a,b]

[a] *School of Biomedical Engineering & Health Sciences, Faculty of Engineering, Universiti Teknologi Malaysia; 81310 UTM Johor Bahru, Johor, Malaysia: and* [b] *IJN-UTM Cardiovascular Engineering Centre, Institute of Human Centered Engineering, Universiti Teknologi Malaysia; 81310 UTM Johor Bahru, Johor, Malaysia.*
Received October 30, 2018; accepted January 21, 2019

Electrodeposition is commonly used to deposit ceramic or metal coating on metallic implants. Its utilization in depositing polymer microcapsule coating is currently being explored. However, there is no encapsulation of drug within polymer microcapsules that will enhance its chemical and biological properties. Therefore, in this study, ginseng which is known for its multiple therapeutic effects was encapsulated inside biodegradable poly(lactic-*co*-glycolic acid) (PLGA) microcapsules to be coated on pre-treated medical grade stainless steel 316L (SS316L) using an electrodeposition technique. Polyaniline (PANI) was incorporated within the microcapsules to drive the formation of microcapsule coating. The electrodeposition was performed at different current densities (1–3 mA) and different deposition times (20–60 s). The chemical composition, morphology and wettability of the microcapsule coatings were characterized through attenuated total reflectance-Fourier transform infrared spectroscopy (ATR-FTIR), scanning electron microscopy (SEM) and contact angle analyses. The changes of electrolyte colors, before and after the electrodeposition were also observed. The addition of PANI has formed low wettability and uniform microcapsule coatings at 2 mA current density and 40 s deposition time. Reduction in the current density or deposition time caused less attachment of microcapsule coatings with high wettability records. While prolonging either one parameter has led to debris formation and melted microcapsules with non-uniform wettability measurements. The color of electrolytes was also changed from milky white to dark yellow when the current density and deposition time increased. The application of tolerable current density and deposition time is crucial to obtain a uniform microcapsule coating, projecting a controlled release of encapsulated drug.

Key words electrodeposition; microcapsule coating; poly(lactic-*co*-glycolic acid); *Panax ginseng*; polyaniline

Introduction

The fast-pace technologies have improved the performance of metallic implants. Several existing metals are verified to be used as metallic implants such as stainless steels, cobalt-based alloys, titanium-based alloys and others (*e.g.*, nitinol and alloys of Mg and Ta) due to its capability to present long-term success in implantation without causing harm to living tissues.[1,2] The outcomes of implant restoration depend primarily on surface chemistry, mechanical durability and biocompatibility of implant materials.[3] Another strategy to improve the outcomes of implant restoration is the utilization of polymer as a coating material.[4] For example, drug/antibacterial polymer based coatings which composed of various types of biodegradable polymers such as polyethylene glycol (PEG),[5] poly(lactic-*co*-glycolic acid) (PLGA).[6,7] and poly(L-lactide) (PLLA)[8] have been coated on metallic implants to control the release of drugs and antibacterial agents.

PLGA is one of the most common used polymers to coat metallic implants.[9] It is a linear copolymer, composed of two constituent monomers which are poly(lactic acid) (PLA) and poly(glycolic acid) (PGA).[9] PLGA has been extensively used in many applications such as implantable matrices and substrates for drug or macromolecules delivery and as a scaffold for tissue engineering[10,11] due to its good biocompatibility[9] and degradability.[12] It has been permitted by Food and Drug Administration (FDA) to be used in human.[11] In this study, PLGA was used to encapsulate an herbal compound of ginseng for drug delivery purpose. Ginseng is classified as a therapeutic compound that can maintain homeostasis of the human body and able to strengthen vital energy.[13,14] An original ginseng or also known as *Panax ginseng* is a small, shade-loving, perennial shrub which belongs to the ivy family *Araliaceae*.[14] Ginseng is being used worldwide, especially in Asian countries for their effects on anti-fatigue,[13] immune system[15] and cardiovascular disease.[16,17] Numerous studies are focused on individual ginsenosides due to strong pharmacological effects of each constituent.

There are several strategies or techniques to coat metallic implants such as dip-coating,[18] thermal spraying and electrophoretic deposition.[19–21] Each technique possesses various advantages while also having disadvantages based on the coating process. For example, a dip-coating technique is able to coat complex structure, permit a mixture of distinct layer of polymers and active principle amounts as well as low cost.[18] However, it could lead to several complications such as bridging, pooling, reduces coating uniformity and produces burst release effect.[22] While a thermal spraying technique such as plasma spray, has high deposition rate but requires advance instrument with an adaptation of high processing temperature.[19] The formation of amorphous coating due to

* To whom correspondence should be addressed. e-mail: syafiqahsaidin@biomedical.utm.my; syafiqahsaidin@gmail.com
© 2019 The Pharmaceutical Society of Japan

rapid cooling from high processing temperature has affected the coating structure and homogeneity.[19,20] The high processing temperature also did not allow polymer coating deposition due to melting and glass transition effects.[23] Therefore, in this study, an electrodeposition technique was employed to form a polymer based coating as it does not require high processing temperature.

Electrodeposition or electrophoretic deposition is another variation of coating technique which has an ability to coat complex geometries and it is preferable for deposition of polymers and biomolecules.[21] This coating technique is inexpensive, fast and simple to deposit layers of material onto metallic implants.[24,25] It has capability to form coating on large surface area and has enormous opportunities in various medical applications such as biosensor, medical device coating and biological scaffold.[26] The process offers high deposition rates and possibility to deposit coating materials onto complex shape substrate such as blood vessel stent[27] and it does not employ chemical cross-linking agent that may cause cells toxicity.[28] Theoretically, deposition of non-conductive polymers using an electrodeposition technique demands integration of conductive materials such as polyaniline (PANI) to drive the formation of polymer based coating. PANI or known as aniline black possesses interesting electrochemical properties with exceptional conduction mechanism.[29] It exists in many forms such as fully oxidized pernigraniline base, half-oxidized emeraldine base and fully reduced leucoemeraldine base.[30] Several researchers have clarified its biocompatibility on different types of cells through cytotoxicity, cells attachment and proliferation analyses.[31–33] However, higher composition of PANI might lead to adverse effects on cell viability.[34,35]

Previously, electrodeposition technique has been used to deposit PLGA microcapsules without fusion of drugs[4] while drugs are necessary to improve chemical and biological properties of the coating.[36,37] Therefore, in this study, ginseng which is known for multiple therapeutic effects, was encapsulated within biodegradable PLGA microcapsules to be deposited on medical grade stainless steel 316L (SS316L) at different current densities and deposition times. The incorporation of PANI inside the coating materials was intended to drive the formation of non-conductive ginseng encapsulated PLGA microcapsules. The chemical composition, morphological and wettability of the coating were characterized principally by using an attenuated total reflectance-Fourier transform infrared spectroscopy (ATR-FTIR), scanning electron microscopy (SEM) and contact angle analyses, respectively. The color changes of electrolyte, before and after the deposition process were also observed and analyzed.

Experimental

Materials Poly(lactic-*co*-glycolic acid) with a lactide/glycolide ratio of 85 : 15 and inherent viscosity of 0.63 dL/g was purchased from LACTEL Absorbable Polymers, U.K. While ginseng extract was supplied by Dalian Hongjiu Biotech, China. Polyaniline (emeraldine base) with a molecular weight of 20000 and sodium chloride (NaCl) were obtained from Sigma-Aldrich, U.S.A. A fully hydrolyzed polyvinyl alcohol (PVA) with a molecular weight of 30000, dichloromethane (DCM) and 30% hydrogen peroxide (H_2O_2) were acquired from Merck KGaA, Germany. Acetone, methanol, glycerol, phosphoric acid (H_3PO_4), nitric acid (HNO_3) and hydrofluoric acid (HF) were purchased from Friendemann Schmidt, Western Australia. A thin foil medical grade SS316L with a thickness of 0.25 mm was purchased from Goodfellow Cambridge Limited, Huntingdon, England.

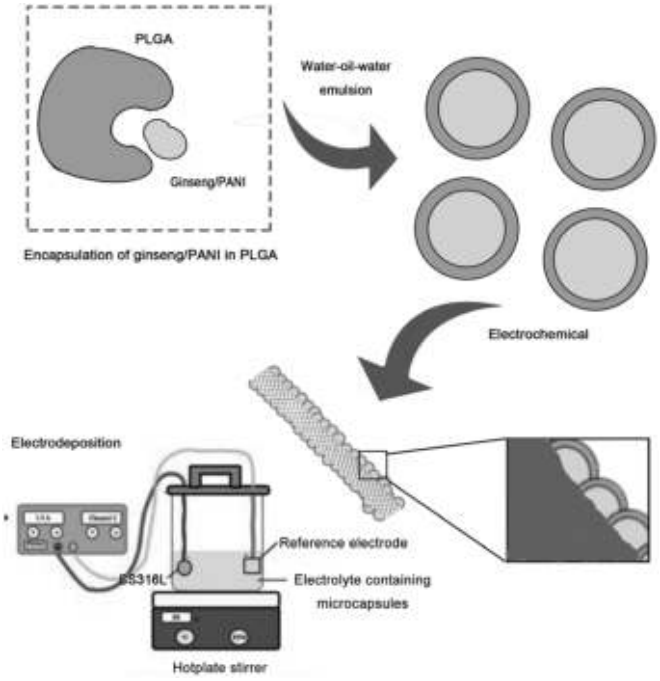

Fig. 1. Schematic Diagram of Ginseng Encapsulation Process and Coating Electrodeposition

Microcapsules Formation Ginseng/PANI was encapsulated in PLGA microcapsules through a double emulsion solvent evaporation method.[38] A mixture of 400 mg of PLGA and 1 mg of PANI were dissolved in 10 mL of DCM. While, 30 mg of ginseng extract was dissolved in 1 mL of distilled (DI) water, separately. Both suspensions were emulsified by a homogenizer at 20000 rpm and 6 min in an ice bath to produce water-in-oil (w/o) emulsion. The w/o emulsified mixture was injected into 60 mL of 1.25% (w/v) PVA solution and continuously homogenized for 10 min at 20000 rpm in an ice bath to achieve water-in-oil-in-water (w/o/w) emulsion.

The DCM was evaporated by stirring the mixture overnight at room temperature. The resulting mixture containing microcapsules was centrifuged at 4°C and 10000 rpm for 30 min. The microcapsules were collected, washed once with 0.9% NaCl, washed twice with DI water and stored at 5°C for further use. The encapsulation process was repeated to encapsulate ginseng inside PLGA microcapsules as a control without the addition of PANI.

Coating Electrodeposition The SS316L foil was cut into 10×10 mm square shape and undergoes several pre-treatment processes[39] which consisted of ultrasonic cleaning, electropolishing and etching. The metals were ultrasonic cleaned in acetone, DI water and methanol for 10 min. Then, the metals were electropolished at 1.5 A for 3 min in an electrolyte solution composed of 50% glycerol, 35% H_3PO_4 and 15% DI water. Etching was performed by dipping the metals in a mixture of 10% HNO_3, 2% HF and 88% DI water for 30 s to remove the remaining adhered electropolishing ions. The pretreated metals were rinsed with DI water and dried using an air compressor.

Table 1. Deposition of Microcapsules Coating on SS316L at Different Setting of Current Densities and Deposition Times

Samples	Current	Deposition time
PLGA/g	1 mA	20 s
PLGA/g/PN1a	1 mA	20 s
PLGA/g/PN1b	1 mA	40 s
PLGA/g/PN1c	1 mA	60 s
PLGA/g/PN2a	2 mA	20 s
PLGA/g/PN2b	2 mA	40 s
PLGA/g/PN2c	2 mA	60 s
PLGA/g/PN3a	3 mA	20 s
PLGA/g/PN3b	3 mA	40 s
PLGA/g/PN3c	3 mA	60 s

A schematic diagram of ginseng encapsulation process and coating electrodeposition is shown in Fig. 1. The ginseng/PANI encapsulated PLGA microcapsules (PLGA/g/PN) and the ginseng encapsulated PLGA microcapsules (PLGA/g) were coated on the pre-treated metals using an electrodeposition technique following the procedures by Wang *et al.*[26] with several modifications. An electrolyte solution containing microcapsules was prepared by adding 1% (w/v) microcapsules into DI water. The conductivity of the electrolyte was improved with the addition of 0.15 M NaCl and 100 mM H_2O_2. The electrolyte mixture was stirred for 30 min at room temperature.

The electrodeposition of the microcapsules was then conducted in a laminar flow using a direct current (DC) power supply (72-8690A, TENMA, Japan). The pre-treated metal was clipped at the cathode while a reference electrode was used as an anode. Both cathode and anode were immersed in an electrolyte solution at room temperature. The electrodeposition was performed at different current densities (1–3 mA) and different deposition times (20–60 s) as shown in Table 1. Finally, the coated metals were rinsed with DI water and dried using an air compressor before putting in a vacuum desiccator for further analyses. The color of electrolyte solution was observed and analyzed using ImageJ software (ImageJ 1.51k, NIH, U.S.A.) in a gray-scale channel,[40] before and after the electrodeposition.

Coating Characterization ATR-FTIR (Nicoler iD5, Thermo Scientific, U.S.A.) was used to study the coating composition. The analyses were conducted using ZnSe crystal at a scanning resolution of 4 cm^{-1}. The spectra were recorded at 32 average scans within 500 and 4000 cm^{-1} frequency ranges. The microstructure and morphology of the coating was viewed under SEM (Hitachi, TM300, Japan) at a magnification of 3000× using an accelerating voltage of 15 kV. An ultrathin gold film with 5 nm thickness was sputtered on the coating using a vacuum sputter coater (Leica EM ACE200, Leica Microsystems, Germany) to avoid charging during the SEM observations. The wettability of the coating was assessed through a contact angle analysis using a video contact angle instrument (VCA Optima, AST Product Inc., U.S.A.). A droplet of 2 μL DI water was dispensed on the coating surface using a 23 gauge needle. The data were recorded at three different areas to obtain an average value.

Results and Discussion

Chemical Composition Analysis The chemical composition of the pre-treated metal and microcapsule coatings were presented on the ATR-FTIR spectra as shown in Fig. 2. No identical peak was observed on the pre-treated metal as the metal surface was free from obvious functional groups. Similar trend was noticed on the PLGA/g where there was no coating attached on the pre-treated metal. The absence of PANI in the coating material of PLGA/g cause restriction in depositing the microcapsules on the pre-treated metal due to non-conductive property of the microcapsules that disturbed electron flow in the electrolyte solution.

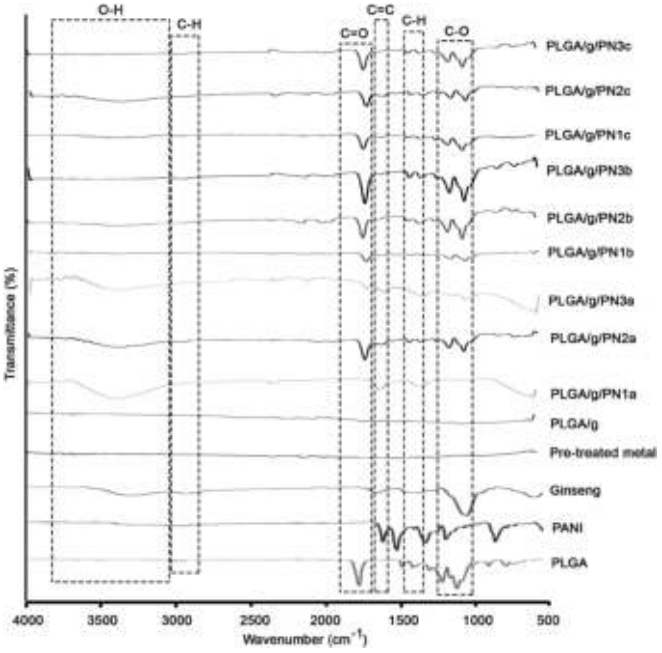

Fig. 2. ATR-FTIR Spectra of Pre-treated Metal, Ginseng Encapsulated PLGA Microcapsule Coatings and Ginseng/PANI Encapsulated PLGA Microcapsule Coatings

While, the other coated metals possesed C–H bending vibration at 1460 cm^{-1}, clarifying the presence of either PLGA or ginseng or both. The existence of C–H functional groups in both materials[11,15] contributed to overlapping of several hydrocarbon peaks between the wavenumber of 1450 and 1470 cm^{-1}. Small peaks of C–H stretching were also noticed approximately at 2900 cm^{-1} on all coated metals except the pre-treated metal and PLGA/g.[41,42] However, another identical peaks of PLGA including carbonyl (C=O) peaks at 1745 cm^{-1} and other identical peaks of PLGA and ginseng including C–O peaks at 1080 and 1187 cm^{-1}, were noticed on all PANI incorporated coatings except the PLGA/g/PN1a. The utilization of 1 mA current density and 20 s deposition time was not enough to drive the ginseng/PANI encapsulated PLGA microcapsules to be deposited on the pre-treated metal.[43]

The appearance of low intensity to medium peaks of C=C stretch alkene was found at 1644 cm^{-1} on all PANI incorporated coatings which attribute the functional group of ginseng. However, another identical peak of ginseng, broad O–H stretching vibration was recorded only on the PLGA/g/PN1a, PLGA/g/PN2a, PLGA/g/PN3a, PLGA/g/PN2b and PLGA/g/PN2c at 3383 cm^{-1}. The electrodeposition using 1 and 3 mA were successful only at 20 s deposition time while the electrodeposition using 2 mA were successful at all deposition times, 20, 40 and 60 s.

The presence of PANI on the coatings could not be clari-

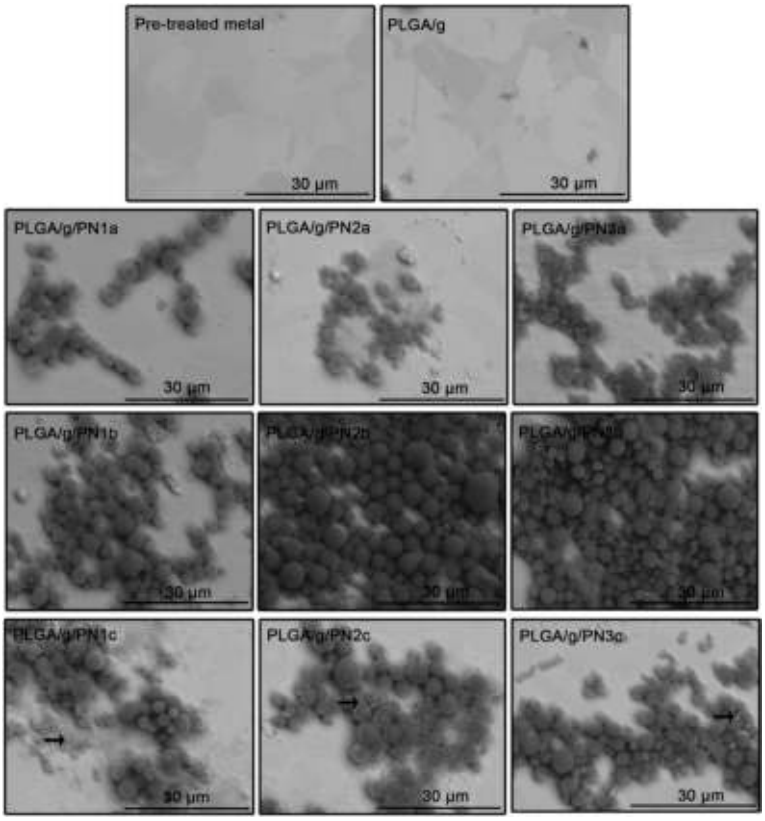

Fig. 3. SEM Images of Pre-treated Metal, Ginseng Encapsulated PLGA Microcapsule Coatings and Ginseng/PANI Encapsulated PLGA Microcapsule Coatings

fied clearly as the C=C, N–H and C–N peaks from the PANI emeraldine compound[32] might be overlapped with other peaks of PLGA and ginseng. For example, the C=C peaks of the PANI in between of 1500 and 1680 cm^{-1} might imbricate the C=C peaks of the ginseng compound. The data require further clarification from other instruments such as X-ray photoelectron spectroscopy to identify specific chemical interaction and chemical bonding. However, in this study, the ATR-FTIR results in Fig. 2 has clearly verified that the incorporation of PANI has initiated the formation of ginseng/PANI encapsulated PLGA microcapsules on the pre-treated metal due to the conductivity property of PANI.

Morphological Structure Analysis The morphology of the pre-treated metal and microcapsule coatings were visualized under SEM as presented in Fig. 3. A smooth pre-treated metal surface is crucial to prevent contamination and to support the attachment of deposited coating.[44] In this study, the macro-dirt was removed during the ultrasonic cleaning process while the passive layer of SS316L was dissolved during the electropolishing process caused the elimination of micro-scratch and flaws on the pre-treated metal. Further treatment of etching was intended to remove the phosphate layer adhered on the metal surface during the electropolishing process.[39] There was no attachment of microcapsules on the PLGA/g. This result supported the data in the ATR-FTIR spectrum of PLGA/g where the absence of PANI has restricted the deposition of microcapsules coating. This incorporated conductive polymer, PANI, is playing an important role in driving the microcapsules to the surface of cathode.

The utilization of PANI has successfully initiated the formation of microcapsule coatings on the pre-treated metal as been visualized in Fig. 3. The ability of PANI to enhance the electro-conductivity property of a material has been proved by Shi *et al.*[45] where the electro-conductivity of bacterial cellulose–PANI composites was increased from 10^{-8} to 10^{-2} S cm^{-1}. However, less coverage of microcapsules coating was noticed when the current density of 1 mA or deposition time of 20 s was applied during the electrodeposition due to insufficient charge or insufficient time to drive the microcapsules onto the pre-treated metal.[43] This result is in accordance with the missing of C–O and C=O peaks in the ATR-FTIR spectrum of PLGA/g/PN1a.

While the deposition time at 40 s has produced more homogenous coating coverage. Prolongation of the deposition time allowed more microcapsules to be deposited on the pre-treated metal. Theoretically, as the time increase, deposition of a new layer will stack on the old deposited layer[44] to develop a thicker microcapsules coating. However, this theory was not achieved at the deposition of 60 s due to debris formation and melted microcapsules as shown by black arrows in the SEM images. The energy was released in the form of heat when long deposition time was applied which resulted in increasing of temperature.[46] The high temperature melted the shell wall of microcapsules, thus releasing the inner core compound.[47]

Wettability Analysis In the perspective of wettability, different application has different preference of wettability surface as cell adhesion and migration can be influenced by the hydrophilic–hydrophobic properties of implant surface.[48] Figure 4 shows the contact angle measurements on the microcapsule coatings deposited on the pre-treated metal at different current densities and deposition times. The maximum wetting was observed on the pre-treated metals which attributed

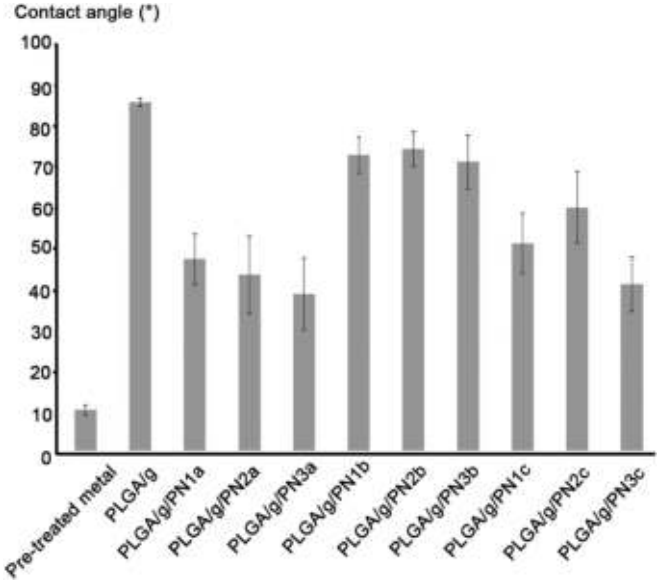

Fig. 4. Contact Angle Measurements on Pre-treated Metal, Ginseng Encapsulated PLGA Microcapsule Coatings and Ginseng/PANI Encapsulated PLGA Microcapsule Coatings

to the removal of thin passivation layers of SS316L, allowing water penetration between the atomic alignments. The wettability was drastically reduced on the PLGA/g surfaces where no microcapsules attachment was observed in the ATR-FTIR and SEM analyses. Therefore, the wettability reduction was contributed by the development of passivation layers on the pre-treated metals during the electrodeposition. This passivation layers were formed due to exposure of the pre-treated metal surfaces to the ambient air and non-polar carbon inside the electrolyte solution.[49,50]

The deposition of ginseng/PANI encapsulated PLGA microcapsule coatings has also reduced the wettability property of the pre-treated metals. The wettability reduction was owing to the hydrophobicity of PLGA instead of the passivation layers of SS316L as the metal surfaces were covered by the PLGA microcapsule coatings. The higher ratio of lactide to glycolide (85 : 15) in the PLGA composition with the presence of methyl side groups in the lactide compound has reduced the surface wettability.[11] The wettability results may also influenced by the hydrophobicity of the PANI.[43] For stent application, a low wettability implant surface is favored to prevent adhesion of cells and inflammatory molecules that might initiate exasperate inflammation and plaque formation.[7]

The 20 s deposition time (PLGA/g/PN1a, PLGA/g/PN2a and PLGA/g/PN3a) demonstrated higher surface wettability compared to the 40 and 60 s deposition times. Less microcapsules were attached on the pre-treated metals at 20 s deposition time, thus exposing more surface of the pre-treated metals which led to high wettability measurements. When the deposition time was increased to 40 s (PLGA/g/PN1b, PLGA/g/PN2b and PLGA/g/PN3b), the microcapsules were started to attach bulkily on the pre-treated metals, resulting in lower wettability measurements. However, non-stable wettability records were attained during the 60 s deposition time (PLGA/g/PN1c, PLGA/g/PN2c and PLGA/g/PN3c) due to formation of debris and melted microcapsules as reported in the SEM observations. The encapsulated ginseng inside the PLGA microcapsules was released once the microcapsules melted, thus exposing the hydrophilicity of the ginseng.[47,51]

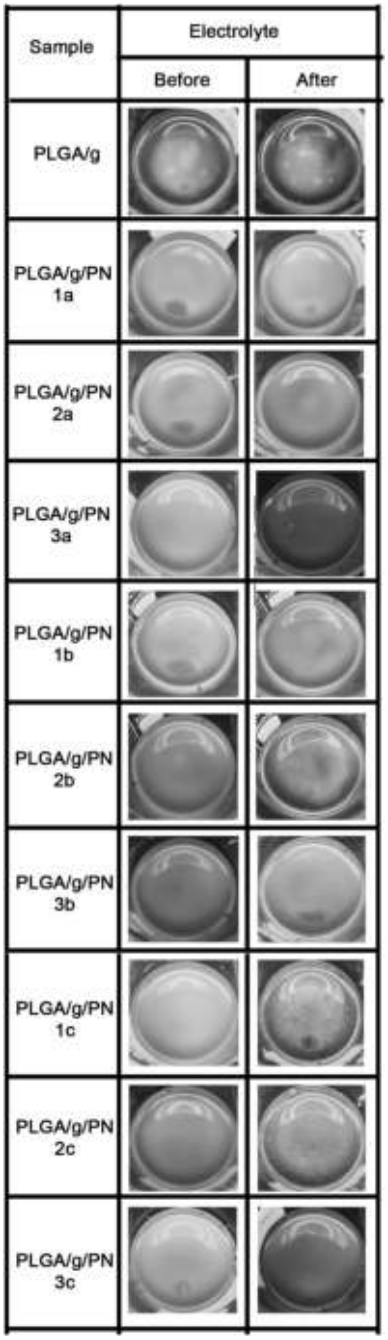

Fig. 5. Color of Electrolyte Solution, before and after Electrodeposition

Color Changes of Electrolyte Figure 5 shows color of electrolyte solution, before and after the electrodeposition. The electrolytes containing ginseng and ginseng/PANI encapsulated PLGA microcapsules were appeared in milky white color. After the electrodeposition, the color of PLGA/g electrolyte was changed to light yellow due to the release of iron (Fe) ions from the SS316L electrode[52] as no microcapsules were attached on the pre-treated metal.

While the color of electrolytes containing ginseng/PANI encapsulated PLGA microcapsules were transiently appeared in darker yellow when the current densities and deposition times increased. The changes in electrolyte color indicated the release of electrode ions and the occurrence of electrochemical reaction within the electrolyte.[43] Faraday's laws of

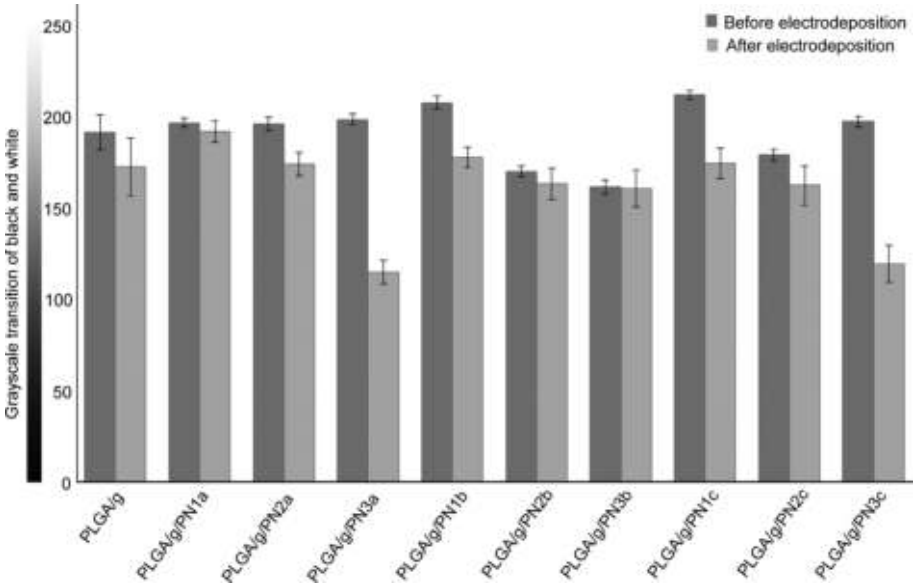

Fig. 6. Quantitative Evaluation of Gray-Scale Channel on Color Changes of Electrolyte Using ImageJ Software

electrolysis[43] explained that the quantity of chemical change yielded by an electrical current is proportional to the amount of current density. In spite of the electrochemical reaction, the release of ginseng from the melted microcapsules could contribute to the changes of electrolyte color.

Figure 6 shows the quantitative evaluation of color changes of electrolyte using ImageJ software in a gray-scale channel based on color intensity and color distribution. The means grayscale were reduced for all electrodeposition parameters after the electrodeposition process, indicate the increment of dark color intensity. These results are in agreement with the appearance of darker yellow electrolytes when the electrodeposition was performed at higher current densities and higher deposition times. The homogeneity of the electrolyte color was then marked by the standard deviation data that stipulates the distribution of analyzed regions. Higher standard deviation values were recorded after the electrodeposition process, correspond to non-homogenous colored electrolyte distribution that came from the release of electrode ions. However, further analysis should be conducted to clarify the composition of electrolyte after the electrodeposition.

Conclusion

The ginseng/PANI encapsulated PLGA microcapsule coatings were deposited on the pre-treated SS316L using an electrodeposition technique at different current densities and deposition times. The electrically conductive polymer, PANI, has served as a positive charge carrier in the electrolyte during the electrodeposition which provided a pathway for deposition of microcapsule coating on the SS316L. A uniform microcapsule coating with low wettability property was obtained at a current density of 2 mA and a deposition time of 40 s. Lower current density (1 mA) or deposition time (20 s) produced less formation of microcapsule coatings due to insufficient applied current and insufficient deposition time. While higher current density (3 mA) or deposition time (60 s) led to melted microcapsules and debris formation due to excessive heat release. This study elucidates the potential utilization of electrodeposition technique to coat a drug/polymer microcapsule coating on metallic implant which would be beneficial to control drug release for medical application.

Acknowledgments The study was supported by Centre of Excellence (CoE) Research Grant [Q.J130000.2445.04G04] and Transdiciplinary Research Grant (TRGS) [R.J130000.7845.4L843], given by Malaysian Ministry of Higher Education (MOHE). The authors also would like to acknowledge Tan Sri Ainuddin Wahid Scholarship.

Conflict of Interest The authors declare no conflict of interest

References

1) Chen Q., Thouas G. A., *Mater. Sci. Eng. Rep.*, **87**, 1–57 (2015).
2) Blackwood D. J., *Corros. Rev.*, **21**, 97–124 (2003).
3) Pradhan D., Wren A. W., Misture S. T., Mellott N. P., *Mater. Sci. Eng. C*, **58**, 918–926 (2016).
4) Nakano K., Egashira K., Masuda S., Funakoshi K., Zhao G., Kimura S., Matoba T., Sueishi K., Endo Y., Kawashima Y., Hara K., Tsujimoto H., Tominaga R., Sunagawa K., *JACC Cardiovasc. Interv.*, **2**, 277–283 (2009).
5) Visan A., Cristescu R., Stefan N., Miroiu M., Nita C., Socol M., Florica C., Rasoga O., Zgura I., Sima L. E., Chiritoiu M., Chifiriuc M. C., Holban A. M., Mihailescu I. N., Socol G., *Appl. Surf. Sci.*, **417**, 234–243 (2017).
6) Carlyle W. C., McClain J. B., Tzafriri A. R., Bailey L., Zani B. G., Markham P. M., Stanley J. R., Edelman E. R., *J. Control. Release*, **162**, 561–567 (2012).
7) Miswan Z., Lukman S. K., Abd Majid F. A., Loke M. F., Saidin S., Hermawan H., *Int. J. Pharm.*, **515**, 460–466 (2016).
8) Bedair T. M., Kang S. N., Joung Y. K., Han D. K., *J. Biomed. Nanotechnol.*, **12**, 2015–2028 (2016).
9) Gentile P., Chiono V., Carmagnola I., Hatton P. V., *Int. J. Mol. Sci.*, **15**, 3640–3659 (2014).
10) Liu R., Huang S. S., Wan Y. H., Ma G. H., Su Z. G., *Colloids Surf. B Biointerfaces*, **51**, 30–38 (2006).
11) Makadia H. K., Siegel S. J., *Polymers*, **3**, 1377–1397 (2011).
12) Costa M. P., Feitosa A. C., Oliveira F. C., Cavalcanti B. C., da Silva E. N., Dias G. G., Sales F. A., Sousa B. L., Barroso-Neto I. L., Pessoa C., Caetano E. W., Di Fiore S., Fischer R., Ladeira L. O., Freire

V. N., *Molecules*, **21**, 873 (2016).
13) Kim H. G., Cho J. H., Yoo S. R., Lee J. S., Han J. M., Lee N. H., Ahn Y. C., Son C. G., *PLOS ONE*, **8**, e61271 (2013).
14) Court W. E., "Ginseng, The Genus Panax," 1st ed., CRC Press, Florida, 2003.
15) Kang S., Min H., *J. Ginseng Res.*, **36**, 354–368 (2012).
16) Kim J. H., *J. Ginseng Res.*, **36**, 16–26 (2012).
17) Lee C. H., Kim J. H., *J. Ginseng Res.*, **38**, 161–166 (2014).
18) Rodríguez-Contreras A., García Y., Manero J. M., Rupérez E., *Eur. Polym. J.*, **90**, 66–78 (2017).
19) Mittal K. L., Etzler F. M., "Adhesion in Pharmaceutical, Biomedical, and Dental Fields," Wiley, New Jersey, 2017.
20) Chakraborty R., Seesala V. S., Sen M., Sengupta S., Dhara S., Saha P., Das K., Das S., *Surf. Coat. Tech.*, **325**, 496–514 (2017).
21) Bosco R., Van Den Beucken J., Leeuwenburgh S., Jansen J., *Coatings*, **2**, 95–119 (2012).
22) Livingston M., Tan A., *J. Med. Devices*, **10**, 010801–010808 (2015).
23) Bush T. B., Khalkhali Z., Champagne V., Schmidt D. P., Rothstein J. P., *J. Therm. Spray Technol.*, **26**, 1548–1564 (2017).
24) Monasterio N., Ledesma J. L., Aranguiz I., Garcia-Romero A., Zuza E., *Surf. Coat. Tech.*, **319**, 12–22 (2017).
25) Furko M., Havasi V., Kónya Z., Grünewald A., Detsch R., Boccaccini A. R., Balázsi C., *Bol. Soc. Esp. Ceram. V.*, **57**, 55–65 (2018).
26) Wang Y., Guo X., Pan R., Han D., Chen T., Geng Z., Xiong Y., Chen Y., *Mater. Sci. Eng. C*, **53**, 222–228 (2015).
27) Wang Y., Pang X., Zhitomirsky I., *Colloids Surf. B Biointerfaces*, **87**, 505–509 (2011).
28) Zhao Y., Liu H., Wang Z., Zhang Q., Li Y., Tian W., Tong Z., Wang Y., Huselstein C., Shi X., Chen Y., *Colloids Surf. B Biointerfaces*, **163**, 412–418 (2018).
29) Abd Razak S. I., Wahab I. F., Fadil F., Dahli F. N., Md Khudzari A. Z., Adeli H., *Adv. Mater. Sci. Eng.*, **2015**, 1–19 (2015).
30) Balint R., Cassidy N. J., Cartmell S. H., *Acta Biomater.*, **10**, 2341–2353 (2014).
31) Prabhakar P. K., Raj S., Anuradha P. R., Sawant S. N., Doble M., *Colloids Surf. B Biointerfaces*, **86**, 146–153 (2011).
32) Kim H. S., Hobbs H. L., Wang L., Rutten M. J., Wamser C. C., *Synth. Met.*, **159**, 1313–1318 (2009).
33) Liu S., Wang J., Zhang D., Zhang P., Ou J., Liu B., Yang S., *Appl. Surf. Sci.*, **256**, 3427–3431 (2010).
34) Moutsatsou P., Coopman K., Georgiadou S., *Polymers*, **9**, 687 (2017).
35) Ma X., Ge J., Li Y., Guo B., Ma P. X., *RSC Adv.*, **4**, 13652–13661 (2014).
36) Singh B. N., Singh B. R., Gupta V. K., Kharwar R. N., Pecoraro L., *Trends Biotechnol.*, **36**, 1103–1106 (2018).
37) Goldberg M., Langer R., Jia X., *J. Biomater. Sci. Polym. Ed.*, **18**, 241–268 (2007).
38) Lukman S. K., Saidin S., Lo Z. K., Al-Ashwal R. H., Based on paper presented at the proceedings of the 2017 international conference on computational biology and bioinformatics, Newark, NJ, U.S.A., 2017, pp. 101–104.
39) Haïdopoulos M., Turgeon S., Sarra-Bournet C., Laroche G., Mantovani D., *J. Mater. Sci. Mater. Med.*, **17**, 647–657 (2006).
40) Beycioğlu A., Çomak B., Akçaabat D., *Acta Phys. Pol. A*, **132** (3-II), 1142–1144 (2017).
41) D'Avila Carvalho Erbetta C, Alves R. J., Resende J. M., de Souza Freitas R. F., de Sousa R. G., *J. Biomater. Nanobiotechnol.*, **3**, 208–225 (2012).
42) Cavalu S. Pînzaru S. C., *Romanian. J. Biophys.*, **15**, 61–66 (2005).
43) Kumar S., Pande S., Verma P., *Int. J. Curr. Eng. Technol.*, **5**, 700–703 (2015).
44) Isa N. N. C., Mohd Y., Zaki M. H. M., Mohamad S. A. S., *Int. J. Electrochem. Sci.*, **12**, 6010–6021 (2017).
45) Shi Z., Zang S., Jiang F., Huang L., Lu D., Ma Y., Yang G., *RSC Advances*, **2**, 1040–1046 (2012).
46) Yue G., Zhang S., Zhu Y., Lu X., Li S., Li Z., *AIChE J.*, **55**, 783–796 (2009).
47) Esser-Kahn A. P., Odom S. A., Sottos N. R., White S. R., Moore J. S., *Macromolecules*, **44**, 5539–5553 (2011).
48) Ghasemi-Mobarakeh L., Prabhakaran M. P., Morshed M., Nasr-Esfahani M. H., Ramakrishna S. H., *Tissue Eng. Part A*, **15**, 3605–3619 (2009).
49) Kietziga A. M., Mirvakilia M. N., Kamalb S., Englezosa P., Hatzikiriakosa S. G., *J. Adhes. Sci. Technol.*, **25**, 1293–1303 (2011).
50) Moradi S., Hadjesfandiari N., Toosi S. F., Kizhakkedathu J. N., Hatzikiriakos S. G., *ACS Appl. Mater. Interfaces*, **8**, 17631–17641 (2016).
51) Rosen M., "Delivery System Handbook for Personal Care and Cosmetic Products: Technology, Applications and Formulations," 1st ed., Elsevier Science, Amsterdam, 2005.
52) Nazneen F., Galvin P., Arrigan D. W. M., Thompson M., Benvenuto P., Herzog G., *J. Solid State Electrochem.*, **16**, 1389–1397 (2012).